AIP | Journal of Applied Physics

Thermodynamics and ferroelectric properties of KNbO3

Linyun Liang, Y. L. Li, Long-Qing Chen, S. Y. Hu, and Guang-Hong Lu

Citation: J. Appl. Phys. **106**, 104118 (2009); doi: 10.1063/1.3260242
View online: http://dx.doi.org/10.1063/1.3260242
View Table of Contents: http://jap.aip.org/resource/1/JAPIAU/v106/i10
Published by the American Institute of Physics.

Thermodynamics and ferroelectric properties of $KNbO_3$

Linyun Liang,[1] Y. L. Li,[2] Long-Qing Chen,[3] S. Y. Hu,[2] and Guang-Hong Lu[1,a)]
[1]*Department of Physics, Beijing University of Aeronautics and Astronautics, Beijing 100191, China*
[2]*Pacific Northwest National Laboratory, Richland, Washington 99352, USA*
[3]*Department of Materials Science and Engineering, The Pennsylvania State University, Pennsylvania 16802, USA*

(Received 3 July 2009; accepted 17 October 2009; published online 24 November 2009)

The Landau–Ginzburg–Devonshire phenomenological theory is employed to model and predict the ferroelectric phase transitions and properties of single-domain potassium niobate ($KNbO_3$). Based on the LGD theory and the experimental data of $KNbO_3$ single crystal, an eighth-order polynomial of free energy function is proposed. The fitted coefficients are validated by comparing to a set of experimental measured values including phase transition temperatures, spontaneous polarization, dielectric constants, and lattice constants. The effects of hydrostatic pressure and external electric field on phase transition temperatures and piezoelectric coefficients are investigated. The free energy function may be used to predict ferroelectric domain structures and properties of $KNbO_3$ bulk and films by phase-field approach. © *2009 American Institute of Physics*. [doi:10.1063/1.3260242]

I. INTRODUCTION

Potassium niobate ($KNbO_3$) has been intensively investigated due to their large electro-optical coefficients, nonlinear optical coefficients, and electromechanical coupling factor for various electronic device applications.[1–4] $KNbO_3$ is also lead-free and environmentally friendly as compared to the widely used lead zirconate titanate (PZT) system.[5,6] At high temperature, $KNbO_3$ is paraelectric with a cubic structure. As temperature decreases, a $KNbO_3$ crystal undergoes a series of ferroelectric phase transitions, i.e., from cubic to tetragonal phases at 435 °C, tetragonal to orthorhombic at 225 °C, and orthorhombic to rhombohedral at −50 °C. At room temperature, $KNbO_3$ has orthorhombic symmetry with the space group *Bmm*2. All of these ferroelectric phase transitions are first-order and involve thermal hysteresis as a result of the lattice deformation and the shift of Nb ion involved in the transitions.

The ferroelectric phase transition behavior of $KNbO_3$ single crystal is quite analogous to $BaTiO_3$. The Landau–Ginzburg–Devonshire (LGD) phenomenological theory has been successfully used to explain the ferroelectric transitions and properties of ferroelectric single crystal like $BaTiO_3$.[7–9] There have also been a number of efforts to develop a LGD phenomenology theory for $KNbO_3$. Cross *et al.*[10] applied a six-order polynomial expression of free energy to determine the order of the ferroelectric-paraelectric phase transition, while the energy coefficients of α_1, α_{11}, and α_{111} were evaluated for the tetragonal phase. Triebwasser[11] also used a six-order free energy function to describe the observed dielectric constant, spontaneous polarization, and latent heat at the paraelectric to ferroelectric transition point by assuming α_{11}, α_{111} to be temperature independent. The energy function coefficients were determined from the experimentally measured dielectric constant and spontaneous polarization values. These thermodynamic models provide a reasonable description for the cubic to tetragonal transition. Kvyatkovski ĭ and Zakharov[12] applied a first-principles method to obtain the energy expansion coefficients by employing the Devonshire–Barrett one-ion model. The Curie temperature and Curie–Weiss constant were calculated. Kleemann and Schäfer[13] applied Landau theory to calculate the entropy and latent heat change at the paraelectric to ferroelectric transition point. Dorfman *et al.*[14] presented a mean-field approach based on the application of the time-dependent Ginzburg–Landau theory to investigate the movement of interphase boundary under applied pressure. However, despite these efforts, the previous free energy functions can only be used to simulate the ferroelectric properties of $KNbO_3$ in the tetragonal phase that is above 225 °C. For the orthorhombic and rhombohedral phases below 225 °C, to our knowledge, no such free energy function has been reported so far. Also lots of experimental data obtained at low temperature, e.g., at room temperature, cannot be reproduced or compared with the calculation results obtained by using these free energy functions. So there is still a lack of a free energy function that accounts for all the ferroelectric phases and phase transitions. Thus, for the benefit of describing the structural and ferroelectric transition for single crystal $KNbO_3$ in the whole phase transition temperature range using thermodynamic phenomenological theory, a more complete description for the free energy function is required.

A phase transition may be influenced by adjusting the external thermodynamic parameters, such as temperature, external fields, and composition. Many prior studies have been focused on the ferroelectric behavior under pressure using various experimental techniques.[14–19] One of the most pronounced pressure effects on the ferroelectric properties is the large shift of the ferroelectric transition temperature.[20] Pressure may modify the characteristics of a phase transition by weakening the first-order transition.[21,22] For optical and piezoelectric applications, e.g., 180° domain pairs can be created by applying electric field.[23] Piezoelectric coefficients

a)Author to whom correspondence should be addressed. Electronic mail: lgh@buaa.edu.cn.

will be significantly enhanced by engineering the domain structure. However, because of the difficulty in the growth of single crystal with sufficient electrical resistance and in poling, there are only a few reports for the piezoelectric properties of $KNbO_3$.[24] The LGD theory will allow one to calculate the properties under applied electric field and pressure.

The main objective of this work is to develop a thermodynamic free energy function by reproducing the experimental properties of the bulk $KNbO_3$ throughout the temperature range. The main results of this work have been briefly introduced in a previous letter.[25] In this paper, the ferroelectric phenomenological theory, free energy function determination, and the applications of the $KNbO_3$ single crystal are described in detail. Additional results and applications including the spontaneous strain, dielectric constants under the hydrostatic pressure, and piezoelectric coefficients under the applied electric field are presented. In the next section (Sec. II), the phenomenological theory of ferroelectricity is given. In Sec. III, the fitting procedure for coefficients of the free energy function is provided. In Sec. IV, coefficient values are evaluated by comparing to experiments. In Sec. V, the properties under the applied hydrostatic pressure and the electric field are calculated based on the fitted energy function as well as the comparison with the related experiments. Finally, a summary is provided in Sec. VI.

II. FERROELECTRIC PHENOMENOLOGICAL THEORY

A. Thermodynamic free energy function

In the LGD phenomenological theory, the spontaneous polarization $\boldsymbol{P}=(P_1,P_2,P_3)$ in a rectangular coordinate system is chosen as the primary order parameter. In this work, an eighth-order polynomial is used to describe the thermodynamics of $KNbO_3$ single crystal. Under stress-free condition, the eight-order polynomial expression is given as[26]

$$\begin{aligned} f_{\mathrm{LGD}}(P_1,P_2,P_3) &= \alpha_1(P_1^2+P_2^2+P_3^2)+\alpha_{11}(P_1^4+P_2^4+P_3^4) \\ &+ \alpha_{12}(P_1^2P_2^2+P_2^2P_3^2+P_1^2P_3^2)+\alpha_{111}(P_1^6+P_2^6 \\ &+ P_3^6)+\alpha_{112}[P_1^4(P_2^2+P_3^2)+P_2^4(P_1^2+P_3^2) \\ &+ P_3^4(P_1^2+P_2^2)]+\alpha_{123}P_1^2P_2^2P_3^2+\alpha_{1111}(P_1^8 \\ &+ P_2^8+P_3^8)+\alpha_{1112}[P_1^6(P_2^2+P_3^2)+P_2^6(P_1^2 \\ &+ P_3^2)+P_3^6(P_1^2+P_2^2)]+\alpha_{1122}(P_1^4P_2^4+P_2^4P_3^4 \\ &+ P_1^4P_3^4)+\alpha_{1123}[P_1^4P_2^2P_3^2+P_2^4P_1^2P_3^2 \\ &+ P_3^4P_1^2P_2^2], \end{aligned} \tag{1}$$

where α with subscript index represents energy expansion coefficient. All of these coefficients are assumed to be temperature independent except α_1, which is assumed to be linearly dependent on temperature and obeys the Curie–Weiss law,

$$\alpha_1=(T-\theta_0)/2\varepsilon_0C_0, \tag{2}$$

where θ_0 is the Curie–Weiss temperature, ε_0 is the permittivity of free space, and C_0 is the Curie constant.

To perform the thermodynamic analysis of $KNbO_3$, polarization is assumed to be $\boldsymbol{P}=(0,0,P_3)$ for the tetragonal phase, $\boldsymbol{P}=(P_3,0,P_3)$ for the orthorhombic phase, and $\boldsymbol{P}=(P_3,P_3,P_3)$ for the rhombohedral phase. At the paraelectric cubic state, $\boldsymbol{P}=(0,0,0)$. Then free energy density of each phase is then simplified to

$$\begin{aligned} f_C &= 0, \\ f_T &= \alpha_1P_3^2+\alpha_{11}P_3^4+\alpha_{111}P_3^6+\alpha_{1111}P_3^8, \\ f_O &= 2\alpha_1P_3^2+(2\alpha_{11}+\alpha_{12})P_3^4+2(\alpha_{111}+\alpha_{112})P_3^6 \\ &+ (2\alpha_{1111}+2\alpha_{1112}+\alpha_{1122})P_3^8, \\ f_R &= 3\alpha_1P_3^2+3(\alpha_{11}+\alpha_{12})P_3^4+(3\alpha_{111}+6\alpha_{112}+\alpha_{123})P_3^6 \\ &+ 3(\alpha_{1111}+2\alpha_{1112}+\alpha_{1122}+\alpha_{1123})P_3^8, \end{aligned} \tag{3}$$

where f, with subscripts C, T, O, and R, represents the free energies of the four phases, respectively, and the energy of the cubic phase is assumed to be zero and used as a potential energy reference point.

The dielectric stiffness coefficient χ_{ij} can be obtained via the second partial derivative of the energy function,

$$\chi_{ij}=\partial^2 f_{\mathrm{LGD}}/\partial P_i\,\partial P_j. \tag{4}$$

Therefore, for the tetragonal phase, the dielectric stiffness coefficients χ_{ij} are

$$\begin{aligned} \chi_{11T} &= \chi_{22T}=2[\alpha_1+\alpha_{12}P_3^2+\alpha_{112}P_3^4+\alpha_{1112}P_3^6], \\ \chi_{33T} &= 2[\alpha_1+6\alpha_{11}P_3^2+15\alpha_{111}P_3^4+28\alpha_{1111}P_3^6], \\ \chi_{12T} &= \chi_{13T}=\chi_{23T}. \end{aligned} \tag{5}$$

For the orthorhombic phase,

$$\begin{aligned} \chi_{11O} &= \chi_{33O}=2[\alpha_1+(6\alpha_{11}+\alpha_{12})P_3^2+(15\alpha_{111} \\ &+ 7\alpha_{112})P_3^4+2(14\alpha_{1111}+8\alpha_{1112}+3\alpha_{1122})P_3^6], \\ \chi_{22O} &= 2[\alpha_1+2\alpha_{12}P_3^2+(2\alpha_{112}+\alpha_{123})P_3^4+2(\alpha_{1112} \\ &+ \alpha_{1123})P_3^6], \\ \chi_{13O} &= 4[\alpha_{12}P_3^2+4\alpha_{112}P_3^4+2(3\alpha_{1112}+2\alpha_{1122})P_3^6], \\ \chi_{12O} &= \chi_{23O}=0. \end{aligned} \tag{6}$$

For the rhombohedral phase,

$$\begin{aligned} \chi_{11R} &= \chi_{22R}=\chi_{33R}=2[\alpha_1+(6\alpha_{11}+2\alpha_{12})P_3^2+(15\alpha_{111} \\ &+ 14\alpha_{112}+\alpha_{123})P_3^4+4(7\alpha_{1111}+8\alpha_{1112}+3\alpha_{1122} \\ &+ 2\alpha_{1123})P_3^6], \\ \chi_{12R} &= \chi_{13R}=\chi_{23R}=4[\alpha_{12}P_3^2+(4\alpha_{112}+\alpha_{123})P_3^4 \\ &+ (6\alpha_{1112}+4\alpha_{1122}+5\alpha_{1123})P_3^6]. \end{aligned} \tag{7}$$

The multiplication by the permittivity of free space ε_0 in Eqs. (4)–(7) can convert the absolute dielectric stiffness coefficients into the relative ones.

In the orthorhombic and rhombohedral states, since the polarization is assumed to be along the ⟨101⟩ and ⟨111⟩ directions of the original cubic axes, the resulted dielectric

stiffness tensor is not diagonal. We can set a new coordinate system $[x_1', x_2', x_3']$ to let the new $[001]'$ direction parallel to the polarization direction. The dielectric stiffness tensor will be diagonalized. The relations of dielectric stiffness coefficients between the old and new coordinates are given below. For the orthorhombic phase, the new dielectric stiffness coefficients χ_{ij}' are given by

$$\chi_{22O}' = \chi_{22O}, \quad \chi_{11O}' = \chi_{33O} - \chi_{13O}, \quad \chi_{33O}' = \chi_{33O} + \chi_{13O}, \quad \chi_{12O}' = \chi_{13O}' = \chi_{23O}' = 0. \tag{8}$$

For the rhombohedral phase, χ_{ij}' are

$$\chi_{11R}' = \chi_{22R}' = \chi_{11R} - \chi_{12R}, \quad \chi_{33R}' = \chi_{11R} + 2\chi_{12R}, \quad \chi_{12R}' = \chi_{23R}' = \chi_{31R}' = 0. \tag{9}$$

The dielectric constant tensor ε_{ij} (ε_{ij}') can be calculated from the dielectric stiffness coefficient by

$$\varepsilon_{ij} = \frac{1}{\varepsilon_0}\chi_{ij}^{-1} \quad \left(\varepsilon_{ij}' = \frac{1}{\varepsilon_0}\chi_{ij}'^{-1}\right), \tag{10}$$

where χ_{ij}^{-1} $(\chi_{ij}'^{-1})$ is the reciprocal matrix of the dielectric stiffness coefficients matrix χ_{ij} (χ_{ij}').

The ferroelectric transition due to the shift of Nb ion will cause the lattice deformation and the corresponding spontaneous strain in the $KNbO_3$. When the cell axes is along the pseudocubic direction, the spontaneous strain can be expressed by

$$e_{11}^0 = Q_{11}P_1^2 + Q_{12}(P_2^2 + P_3^2),$$

$$e_{22}^0 = Q_{11}P_2^2 + Q_{12}(P_1^2 + P_3^2),$$

$$e_{33}^0 = Q_{11}P_3^2 + Q_{12}(P_1^2 + P_2^2),$$

$$e_{12}^0 = Q_{44}P_1P_2, e_{13}^0 = Q_{44}P_1P_3, e_{23}^0 = Q_{44}P_2P_3, \tag{11}$$

where Q_{11}, Q_{12}, and Q_{44} are the electrostrictive coefficients that can be measured by experiments.

The lattice constants of three ferroelectric phases can be calculated by

$$a_T = a_0(1 + e_{11T}^0) = a_0(1 + e_{22T}^0), c_T = a_0(1 + e_{33T}^0),$$

$$a_O = c_O = a_0(1 + e_{11O}^0) = a_0(1 + e_{33O}^0), b_O = a_0(1 + e_{22O}^0),$$

$$a_R = a_0(1 + e_{11R}^0) = a_0(1 + e_{22R}^0) = a_0(1 + e_{33R}^0), \tag{12}$$

where a_0 is the pseudocubic lattice constant.

B. Free energy function under constant pressure

The change of the phase transition temperature under applied external stresses can be calculated based on the LGD energy function. Under an external stress $\boldsymbol{\sigma} = (\sigma_1, \sigma_2, \sigma_3, \sigma_4, \sigma_5, \sigma_6)$, the free energy function can be rewritten by

$$f_\sigma = f_{\mathrm{LGD}} - \tfrac{1}{2}s_{11}(\sigma_1^2 + \sigma_2^2 + \sigma_3^2) - s_{12}(\sigma_1\sigma_2 + \sigma_1\sigma_3 + \sigma_3\sigma_2) - \tfrac{1}{2}s_{44}(\sigma_4^2 + \sigma_5^2 + \sigma_6^2) - Q_{11}(\sigma_1P_1^2 + \sigma_2P_2^2 + \sigma_3P_3^2) - Q_{12}[\sigma_1(P_2^2 + P_3^2) + \sigma_2(P_1^2 + P_3^2) + \sigma_3(P_1^2 + P_3^2)] - Q_{44}(P_2P_3\sigma_4 + P_1P_3\sigma_5 + P_2P_1\sigma_6), \tag{13}$$

where s_{11}, s_{12}, and s_{44} are the elastic compliances at the constant polarization. In the hydrostatic pressure condition, the pressure tensors must satisfy $\sigma_1 = \sigma_2 = \sigma_3 = -\sigma$, $\sigma_4 = \sigma_5 = \sigma_6 = 0$. Thus, Eq. (13) becomes

$$f_\sigma = f_{\mathrm{LGD}} - \tfrac{3}{2}s_{11}\sigma^2 - 3s_{12}\sigma^2 + Q_{11}\sigma(P_1^2 + P_2^2 + P_3^2) + 2Q_{12}\sigma[P_1^2 + P_2^2 + P_3^2]. \tag{14}$$

C. Free energy function under an applied electric field

Many useful properties of ferroelectric materials such as the piezoelectric and electrostriction rely on the strain gen-

TABLE I. The thermodynamic parameters used for fitting the LGD energy expansion coefficients.

	Parameter							
	Transition temperature			Dielectric constant				
Symbol	T_{c1} [a]	T_{c2} [a]	T_{c3} [b]	ε_{22} [c]	ε_{33} [c]	ε_{11} [d]	ε_{22} [d]	ε_{33} [d]
Temperature (°C)	⋯	⋯	⋯	227	227	22	22	22
Value	435 °C	225 °C	−50 °C	2089	296	1000	160	55

	Parameter			
	Entropy change	Curie–Weiss temperature	Curie constant	Polarization
Symbol	ΔS_1 [e]	T_0 [f]	C_0 [g]	P_s [f]
Temperature (°C)	435	⋯	⋯	418
Value	29 485.6 J m^{-3} K^{-1}	377 °C	2.4×10^5 °C	0.26 C/m^2

[a]Reference 27.
[b]Reference 28.
[c]Reference 29.
[d]Reference 30.
[e]Reference 31.
[f]Reference 11.
[g]Reference 32.

TABLE II. The fitted LGD energy expansion coefficients for $KNbO_3$ single crystal.

Coefficients	This work	Others[a]	Units
α_1	4.273×10^5 (T-377)	2.173×10^5 (T-377)	$C^{-2}m^2N$
α_{11}	-6.36×10^8	-4.05×10^8	$C^{-4}m^6N$
α_{12}	9.66×10^8	⋯	$C^{-4}m^6N$
α_{111}	2.81×10^9	2.99×10^9	$C^{-6}m^{10}N$
α_{112}	-1.99×10^9	⋯	$C^{-6}m^{10}N$
α_{123}	6.03×10^9	⋯	$C^{-6}m^{10}N$
α_{1111}	1.74×10^{10}	⋯	$C^{-8}m^{14}N$
α_{1112}	5.99×10^9	⋯	$C^{-8}m^{14}N$
α_{1122}	2.50×10^{10}	⋯	$C^{-8}m^{14}N$
α_{1123}	-1.17×10^{10}	⋯	$C^{-8}m^{14}N$

[a]Reference 11.

erated by the applied electric field. With the applied external electric field $E=(E_1,E_2,E_3)$, the LGD energy function is thus rewritten as

$$f_E = f_{\mathrm{LGD}} - E_1P_1 - E_2P_2 - E_3P_3. \tag{15}$$

The piezoelectric coefficient can be obtained through the derivative of strain e_{ij} with respect to the electric field, i.e.,

$$d_{kij} = \frac{de_{ij}}{dE_k} \quad (i,j,k=1,2,3), \tag{16}$$

where d_{kij} is the piezoelectric coefficient and subscripts (i,j,k) denote the crystallographic axes.

III. DETERMINATION OF COEFFICIENTS FOR THE FREE ENERGY FUNCTION

We first fit the coefficients of the free energy function based on the experimental data including transition temperatures, spontaneous polarization, dielectric constants, entropy change, etc., which are listed in Table I. Using these fitted coefficients, we can calculate all the structural and ferroelectric properties to validate these coefficients. In the following, we will show the procedures about how to fit these energy coefficients.

Let us take the cubic to tetragonal phase transition as an example. The energies for the cubic and tetragonal phase at the transition point must be equal. Since we use the cubic phase as the reference for the free energy function, at the cubic to tetragonal transition temperature, it implies

$$f_T = \alpha_1P_3^2 + \alpha_{11}P_3^4 + \alpha_{111}P_3^6 + \alpha_{1111}P_3^8 = 0. \tag{17}$$

The first derivative of energy for the tetragonal phase must be zero at a given spontaneous polarization, i.e.,

$$\partial f_T/\partial P_3 = \alpha_1 + 2\alpha_{11}P_3^2 + 3\alpha_{111}P_3^4 + 4\alpha_{1111}P_3^6 = 0. \tag{18}$$

For describing the properties for the tetragonal phase, α_1 (C_0), α_{11}, α_{111}, α_{1111}, and P_3 should be determined. In order to determine these five quantities, five equations are needed. Based on the experimental spontaneous polarization value of 0.26 C/m^2 for the cubic to tetragonal transition at the temperature 418 °C,[11] we use three different polarizations around this value at three given temperatures to fit these parameters. The fitted parameters are then tested by comparing the predicted ferroelectric properties from the thermodynamic model to experimentally measured values including transition temperatures, dielectric constants, spontaneous polarizations, Curie constant, and entropy change as shown in Table I. We tried many different polarizations to fit the experimental measured values and found that the spontaneous polarizations with 0.33, 0.32, and 0.27 C/m^2 at respective three given temperatures of 250, 300, and 435 °C gave a better fitting.

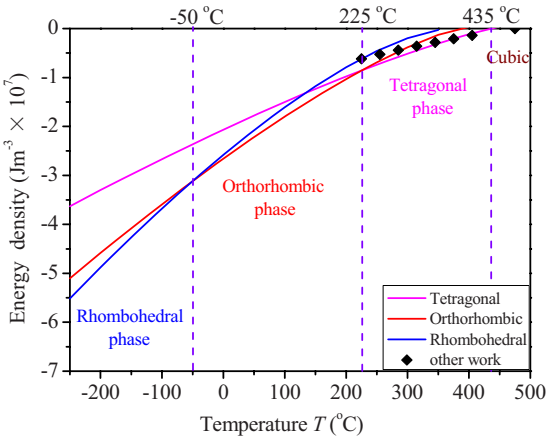

FIG. 1. (Color online) The LGD energy of three ferroelectric phases as a function of temperature. The black squares represent the energy values based on α_{11} and α_{111} from the previous work (Ref. 11).

The entropy change for the cubic paraelectric to tetragonal ferroelectric phase transition is

$$\Delta S = [P^2_{\mathrm{product}}(T_c) - P^2_{\mathrm{parent}}(T_c)]/2\varepsilon_0C_0, \tag{19}$$

where P_{product} is the spontaneous polarization for the product phase and P_{parent} is the polarization for the parent phase at the transition point. The reported experimental value of ΔS is 29 485.6 $Jm^{-3}K^{-1}$ at the equilibrium transition temperature,[31] thus we use Eq. (19) as one of five equations to determine the coefficients of the free energy function. Using Eqs. (17)–(19), all coefficients for the tetragonal phase can be determined uniquely.

With the determination of α_1, α_{11}, α_{111}, and α_{1111}, we are able to fit the rest of free energy coefficients based on the experimental data associated with the orthorhombic and

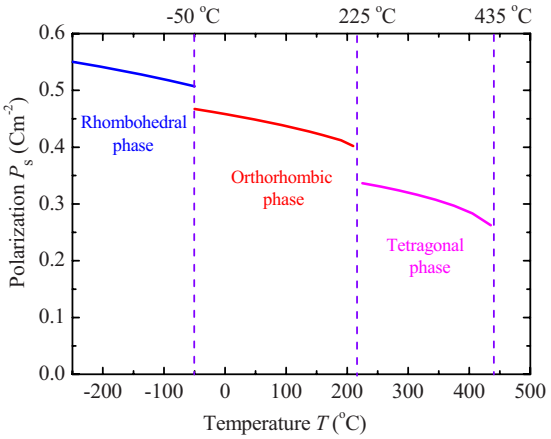

FIG. 2. (Color online) Polarization vs temperature in the $KNbO_3$ single domain, where $P_s=|\mathbf{P}|$, $\boldsymbol{P}=(0,0,P_3)$ in the tetragonal phase, $\boldsymbol{P}=(P_3,0,P_3)$ in the orthorhombic phase, and $\boldsymbol{P}=(P_3,P_3,P_3)$ in the rhombohedral phase.

TABLE III. The values of polarization (C/m^2) and dielectric constant for $KNbO_3$ at room temperature ($T=22$ °C).

Properties	This work	Experiment				
P_s	0.45	0.3347,[a] 0.43[g]	0.41,[b]	0.38,[c]	0.38 ± 0.04,[d]	0.41 ± 0.02,[e] 0.42,[f]

[a]Reference 36.
[b]Reference 30.
[c]Reference 37.
[d]Reference 38.
[e]Reference 24.
[f]Reference 39.
[g]Reference 33.

rhombohedral phases using the similar method as shown above. These experimental data used for fitting and comparing are listed in Table I. All the fitted expansion coefficients of the LGD energy function for $KNbO_3$ single crystal are listed in Table II. The coefficients α_1, α_{11}, and α_{111} obtained by others[11] are also given for comparison.

IV. FERROELECTRIC PROPERTIES CALCULATED FROM THE FITTED COEFFICIENTS FOR THE FREE ENERGY FUNCTION

With the fitted coefficients in Table II, the free energy densities of three ferroelectric phases as a function of polarization are shown in Fig. 1. The actual stable state of the crystal should correspond to the minimum of the free energy of the system. It is clearly shown that the tetragonal phase exhibits lowest energy from 435 to 225 °C while the orthorhombic and rhombohedral phases are energetically most stable from 225 to −50 °C and below −50 °C, respectively. The free energy density of the tetragonal phase from an existing sixth-order polynomial is also included for comparison.[11]

Figure 2 shows the spontaneous polarization dependence on temperature. One can see from Fig. 2 that the magnitude of polarizations decreases with increase in temperature and changes abruptly at each transition point, which is characteristic of first-order phase transitions. The spontaneous polarization in the tetragonal state is 0.27 C/m^2 at 435 °C and goes up to 0.34 C/m^2 near the tetragonal to orthorhombic transition point. Existing experimental measurements indicated that the spontaneous polarization in the tetragonal phase might be larger. For example, values of 0.371 (Ref. 33) and 0.396 C/m^2 (Ref. 34) were suggested as compared earlier experimental value of $P_s=0.30$ C/m^2.[11] Kleemann *et al.*[13] confirmed a larger value $P_s=0.373$ C/m^2 at 227 °C by the linear birefringence data. Resta *et al.*[35] used the Bloch functions of the tetragonal phase to calculate the polarization value and obtained $P_s=0.35$ C/m^2 at 270 °C. The value of polarization at room temperature is compared with the experimentally measured data given in Table III. The calculated polarization is 0.45 C/m^2 at the room temperature, in agreement with the other experimental and computational work. The value of polarization is 0.51 C/m^2 at −50 °C in the rhombohedral phase.

The entropy at a transition temperature is discontinuous due to the first-order phase transition characteristics. The entropy changes from the higher to lower temperature phases at three ferroelectric phase transition points are calculated by Eq. (19) and are listed in Table IV. These values are in good agreement with the experimental values.[31]

The latent heat change at the transition point can be calculated by the expression $\Delta L=T_c\Delta S$, where T_c is the phase transition temperature. As shown in Table IV, the latent heat change ΔL is consistent with the experiment.[40,41] These larger latent heat changes in $KNbO_3$ can be attributed to the large lattice distortions.

The dielectric constant is one of the important properties of the ferroelectric $KNbO_3$ single crystal. Figure 3 shows the dielectric constant tensors in three ferroelectric phases, which are calculated through Eq. (10). Experimental values[29] are also shown in the figure for comparison. The plotted dielectric constant ε_{33} (ε'_{33}) is along the polar direction, while ε_{11} (ε'_{11}) and ε_{22} (ε'_{22}) are along the other two directions which are orthogonal to each other and also to the polarization. For the tetragonal phase, ε_{11} agrees well with the experimental values, while ε_{33} is underestimated in comparison with the only experimental data we could find so far. Despite its underestimated absolute value, the ε_{33} variation with the temperature is consistent with experiment. For the orthorhombic phase, ε'_{11}, ε'_{22}, and ε'_{33} are in good agreement with the experimental data. Furthermore, the dielectric constants for the rhombohedral phase are also calculated as shown in Fig. 3, but no experimental data are available for a comparison.

The spontaneous strain is generated accompanying with the phase transition. The spontaneous strains along the crystallographic axes of the pseudocubic can be calculated from

TABLE IV. Entropy S and latent heat L changes of $KNbO_3$ at three ferroelectric phase transition points.

	Properties					
	ΔS			ΔL		
Transition	This work [$J\ m^{-3}\ K^{-1}$]	[cal/(mole K)]	Others[a] [cal/(mole K)]	This work [Jm^{-3}]	[cal/(mole)]	Others[b,c] [cal/(mole)]
Cubic to tetragonal	29 485.6	0.28	0.28	2.1×10^7	196	190 ± 15
Tetragonal to orthorhombic	20 050.9	0.19	0.17	1.5×10^7	93	85 ± 10
Orthorhombic to rhombohedral	16 569.5	0.16	0.12	6.6×10^6	34	32 ± 5

[a]Reference 31.
[b]Reference 40.
[c]Reference 41.

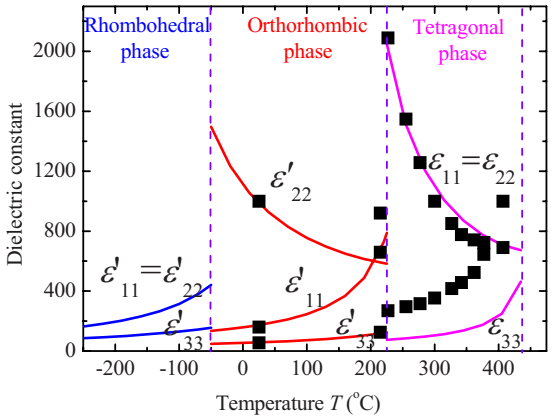

FIG. 3. (Color online) Dielectric constants vs temperature in the $KNbO_3$ single crystal. ε_{33} (ε'_{33}) is along the polarization direction and ε_{11} (ε'_{11}) and ε_{22} (ε'_{22}) are along the two directions orthogonal to the polarization direction. For the tetragonal phase, $\varepsilon_{11}=\varepsilon_{22}$. For the orthorhombic and rhombohedral phases, ε'_{33} is along the [010] and [001] polarization directions. The squares represent the experimental values and the solid lines represent the calculated values by the thermodynamic free energy.

the polarizations, as expressed in Eq. (11). Figure 4 shows the calculated spontaneous strains as a function of the temperature for all the three ferroelectric phases. For the tetragonal phase, the spontaneous polarization is along with the x_3 direction. The spontaneous strain e^0_{11T} is equal to e^0_{22T}, and the spontaneous strain e^0_{33T} along the x_3 direction is larger than e^0_{11T} and e^0_{22T}. In the case of the orthorhombic phase, the spontaneous polarization is along the [101] direction. The spontaneous strain e^0_{11O} is equal to e^0_{33O} while, in the rhombohedral phase case, e^0_{11R} is equal to both e^0_{22R} and e^0_{33R} because the polarization is along the [111] direction. In order to determine the spontaneous strain, we set the electrostrictive coefficients $Q_{11}=0.12$ m^4/C^2, $Q_{12}=-0.053$ m^4/C^2, and $Q_{44}=0.052$ m^4/C^2 instead of the experimentally measured values of $Q_{11}=0.13$ m^4/C^2, $Q_{12}=-0.047$ m^4/C^2, and $Q_{44}=0.052$ m^4/C^2, or $Q_{11}=0.13$ m^4/C^2, $Q_{12}=-0.055$ m^4/C^2, and $Q_{44}=0.052$ m^4/C^2.[10] This is because the phase transition properties under the hydrostatic pressure (see Sec. IV) calculated from these electrostrictive coefficients largely deviate from the experimental values. The calculated spontaneous strain values in the orthorhombic phase are in reasonable agreement with previous studies.

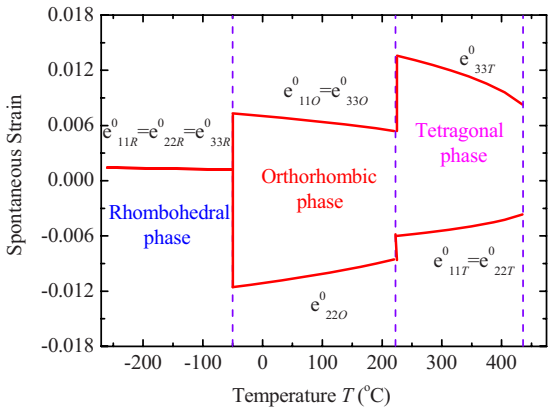

FIG. 4. (Color online) Spontaneous strain as a function of the temperature in $KNbO_3$.

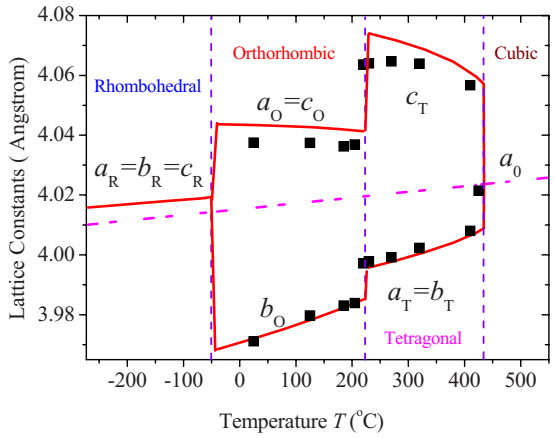

FIG. 5. (Color online) Lattice constant vs temperature in the $KNbO_3$ single crystal. The squares represent experimental values from Ref. 40. The solid lines represent calculated values through the present free energy. The dashed line represents pseudocubic lattice a_0.

The lattice constants in different phases can be determined from the spontaneous strain by Eq. (12). Figure 5 shows the calculated lattice constants of $KNbO_3$ as a function of temperature. The black squares represent experimental values.[40] The lattice constants of three ferroelectric phases, a_T, b_T, and c_T for the tetragonal phase, a_O, b_O, and c_O for the orthorhombic phase, and a_R, b_R, and c_R for the rhombohedral phase, are obtained by Eq. (12), where a_0 is the lattice of the pseudocubic and $a_0=4.015\,29+1.923\,36\times10^{-5}$ T fitted from the cubic data and extrapolated to lower temperature.[40] They are in reasonable agreement with the experimental values. Sepliarsky *et al.*[42] also calculated the lattice constants versus the temperature using the molecular dynamic method, which shows the larger lattice constants in comparison with the present work.

V. EFFECT OF EXTERNAL PRESSURE AND ELECTRIC FIELD

A. Phase transition properties under hydrostatic pressure

Besides temperature, pressure change may lead to the phase transitions. A notable feature of the ferroelectric $KNbO_3$ is the phase-transition temperature shift under an applied pressure. Using the Raman spectroscopic measurement and optical observation, Gourdain *et al.*[22] found that the tetragonal-cubic phase transition occurs at ~9–10 GPa at the room temperature. Shamim and Ishidate[17] analyzed the Raman spectra of $KNbO_3$ under the high pressure and found that the orthorhombic-tetragonal and tetragonal-cubic phase transitions occur at 7 and 8 GPa at room temperature, respectively. Kobayashi *et al.*[19,43] measured the dielectric constant dependence on temperature and pressure in all three ferroelectric phases and gave the phase-transition pressures are 8.5 and 11 GPa at room temperature for the orthorhombic-tetragonal and tetragonal-cubic phase transitions, respectively. Gourdain *et al.*[16] reported a transition pressure of 10–11GPa for the tetragonal-cubic phase transition and 5–7 GPa for the orthorhombic-tetragonal phase transition at room temperature.

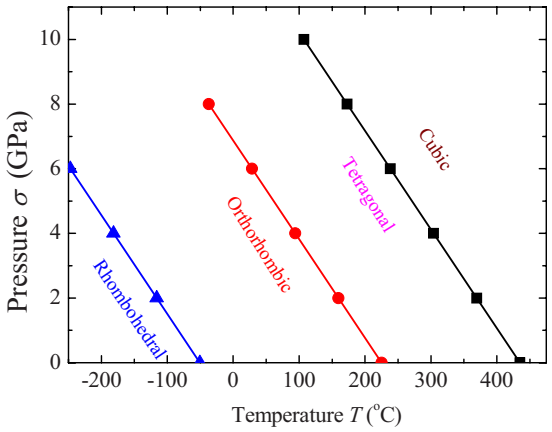

FIG. 6. (Color online) Phase diagram as a function of transition temperature and applied pressure for $KNbO_3$.

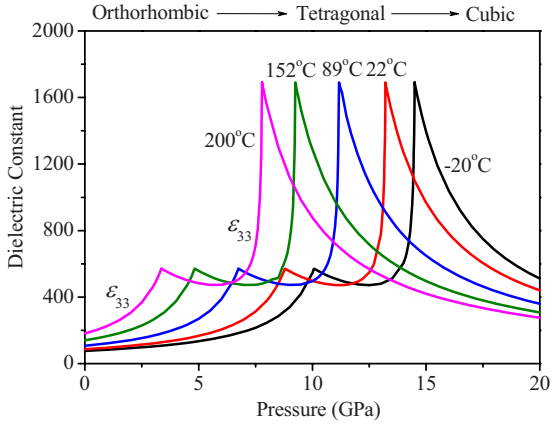

FIG. 7. (Color online) Dependence of the dielectric constant (ε_{33}) of $KNbO_3$ on hydrostatic pressure at different temperatures.

The phase transition temperature under the applied external pressure can be calculated by using Eq. (13). The elastic compliance constants in this calculation are taken as $s_{11}=4.6\times10^{-12}$ m^2/N, $s_{12}=-1.1\times10^{-12}$ m^2/N, and $s_{44}=11.1\times10^{-12}$ m^2/N according to the experiment.[10] The calculation results are shown in Fig. 6. It is found that the cubic-tetragonal phase transition occurs at 12.5 GPa and the orthorhombic-tetragonal transition occurs at 6.1 GPa at room temperature, which is in agreement with experiment. We can estimate the derivative of the pressure σ with respect to the transition temperature through $\partial P/\partial T_c$, which is approximately -0.03 GPa/K for all the three phase transitions of $KNbO_3$. For the tetragonal-cubic phase transition, the predicted value is consistent with the experimental measured value of -0.036 GPa/K.[17] For the orthorhombic-tetragonal phase transition, the calculated value is the same as the experimental data of -0.03 GPa/K by Gourdain *et al.*[16] using x-ray diffraction and Raman scattering measurements. However, we need to point out that the all phase transitions under hydrostatic pressure are the first order transition. It is seen from Eqs. (13) and (14) that the introduction of applied stresses or hydrostatic pressure only affects the coefficients of the second order term of the LGD free energy that does not cause any change on phase transition order. But applied constraint strain can result in phase transition orders.[44,45]

The dielectric constant under an applied pressure can be calculated from Eqs. (4) and (10) where the free energy is replaced by Eq. (14). The spontaneous polarization is still along the $[001]_{pc}$ direction for the tetragonal phase and along the $[101]_{pc}$ direction for the orthorhombic phase. We calculate the dielectric constant tensor ε_{33} along the pseudocubic axis [001] at various hydrostatic pressures under constant temperatures. We chose five temperatures, i.e., -20, 22, 200, and 200 °C, as well as 152 and 89 °C in order to make a comparison with the corresponding experiment. Figure 7 shows the curves of the dielectric constant ε_{33}. As it can be seen in the plot that ε_{33} increases with pressure and exhibits two maxima which correspond to the orthorhombic-tetragonal and tetragonal-cubic phase transition points for the given temperature. Clearly, the orthorhombic-tetragonal phase transition pressures at 152 and 89 °C are 4.8 and 6.8 GPa, while the tetragonal-cubic phase-transition pressures under the same temperatures are 9.2 and 11.2 GPa, respectively, consistent with experiments.[19] We thus can obtain the dielectric constants of $KNbO_3$ under any pressure at different temperatures, most of which are currently unavailable. As shown in Fig. 7, the dielectric constants at the -22, 22, and 200 °C are calculated based on the fitted free energy function. Obviously, the transition pressure decreases as temperature increases, which is consistent with experimental observations.

Figure 8 shows the dielectric constant ε_{33} as a function of the temperature under given hydrostatic pressures. The selected hydrostatic pressures used in the calculations are 2, 4, 6, 8, and 10 GPa. Figure 8 shows the tetragonal-cubic and orthorhombic-tetragonal phase transitions, characterized by the two peaks. Obviously, the transition temperature decreases with the applied hydrostatic pressure, which is consistent with experimental observations.[19] The transition temperatures for the orthorhombic-tetragonal and tetragonal-cubic phase transitions are 277 and 422 °C at 2 GPa, which decrease to -17 and 127 °C at 10 GPa. The ferroelectric transition temperature decreases and the temperature range between the orthorhombic and tetragonal phase is narrowed with increasing pressure. Using the fitted thermodynamic free energy function, we can thus obtain the dielectric constant values at any temperatures and pressures.

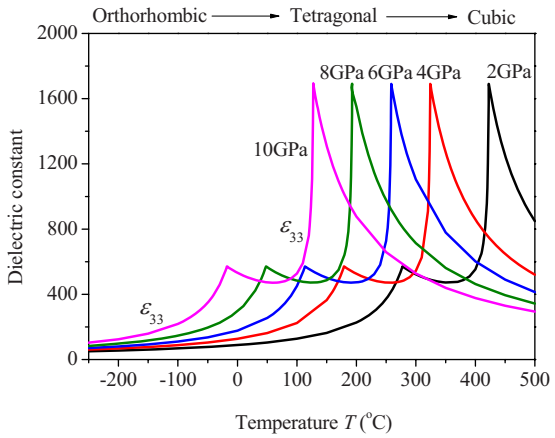

FIG. 8. (Color online) Dependence of the dielectric constant (ε_{33}) $KNbO_3$ on temperature under different hydrostatic pressures.

B. Piezoelectric properties under applied electric field

The piezoelectric coefficients can be calculated through the derivative of strain with respect to the electric field using Eq. (16). We apply the electric fields of $\boldsymbol{E}=(0,0,E_0)$, $\boldsymbol{E}=(E_0,0,E_0)$, and $\boldsymbol{E}=(E_0,E_0,E_0)$ at room temperature. At room temperature under zero electric field, the ferroelectric orthorhombic phase is stable. The corresponding spontaneous polarization is assumed to be along the [101] direction. We calculate the piezoelectric coefficients along the applied electric field directions and the other two directions which are orthogonal to each other and to the electric field direction. We take the engineering notations d_{33}, d_{32}, and d_{31}. For example, for the electric field $\boldsymbol{E}=(E_0,0,E_0)$, the three orthogonal directions are chosen as $[10\bar{1}]$, [010], and [101]. The corresponding piezoelectric constants are calculated as

$$d_{31}=\frac{\partial e_{[10\bar{1}]}}{\partial E_{[101]}},\quad d_{32}=\frac{\partial e_{[010]}}{\partial E_{[101]}},\quad d_{33}=\frac{\partial e_{[101]}}{\partial E_{[101]}}. \tag{20}$$

Under stress-free condition, the strains $e_{[10\bar{1}]}$, $e_{[010]}$, and $e_{[101]}$ are calculated with

$$e_{[l,m,n]}=e_{11}^0l^2+e_{22}^0m^2+e_{33}^0n^2+2e_{12}^0lm+2e_{13}^0ln+2e_{23}^0mn, \tag{21}$$

where $[l,m,n]$ is the direction unit vector with $l^2+m^2+n^2=1$. d_{3i} under the electric field $\boldsymbol{E}=(0,0,E_0)$ and $\boldsymbol{E}=(E_0,E_0,E_0)$ is calculated in the same way. Figure 9 shows the predicted piezoelectric coefficients as a function of applied electric field at room temperature. We checked the stable polarization solutions of the free energy function before calculating the piezoelectric coefficients. It is found that a ferroelectric phase transition occurs when applying the electric field $E_{[111]}$, which is represented by the abrupt change of the piezoelectric constant as shown in Fig. 9(c). The orthorhombic phase changes into rhombohedral phase at the electric field 9.9 MV m^{-1}. It is noted that d_{33} always has the highest values comparing with d_{31} and d_{32}. In addition, d_{33} decreases with the increasing of electric field along [001] and [101] directions, while d_{31} and d_{32} increase. However, there is no significant variation of d_{31}, d_{32}, and d_{33} with the electric field $E_{[001]}$ and $E_{[101]}$ as shown in Figs. 9(a) and 9(b).

The values of piezoelectric coefficients under the electric field $E_{[101]}$ at room temperature are listed in Table V in comparison with other computational and experimental data. Piezoelectric coefficient tensor d_{33} and d_{32} are in good agreement with experiments, while d_{31} is smaller than the experimental values, although the experimental values among themselves also have a large difference. It has been suggested that d_{3i} may be enhanced by using various experimental methods. For instance, Nakamura *et al.*[3] presented the experimental confirmation of the strain versus electric field behaviors of (001) cut $KNbO_3$ with a single-domain structure. The effective piezoelectric coefficient d_{33} was shown to be about 80 pc/N when the direction of electric field was set the same as that of the original spontaneous polarization. Masuda *et al.*[47] reported that the piezoelectric coefficient d_{33} of the electrically poled $KNbO_3$ ceramics by doping La and Fe was 98 pC/N.

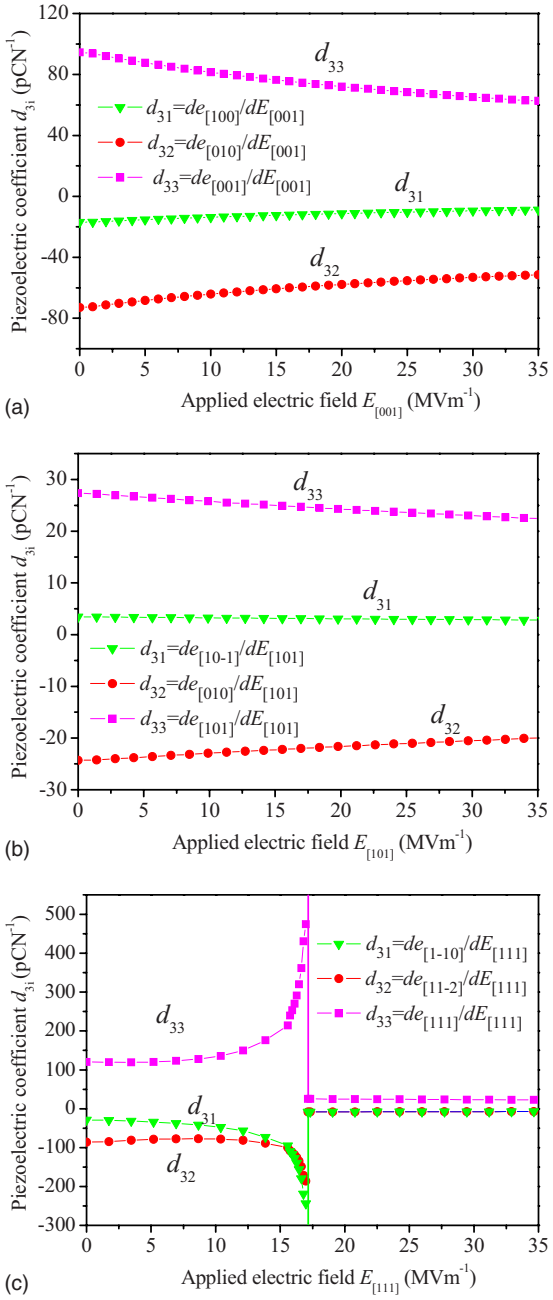

FIG. 9. (Color online) Piezoelectric coefficients vs applied electric field $E_{[001]}=E_0$, $E_{[101]}=\sqrt{2}E_0$, and $E_{[111]}=\sqrt{3}E_0$, respectively, at room temperature.

C. Application of the fitted free energy function in the phase-field method

The phase-field model has been successfully developed as a powerful computational approach for studying mesos-

TABLE V. Piezoelectric coefficients under the applied electric field $E_{[101]}$ at room temperature (T=22 °C).

Properties	This work	Others	Units
d_{33}	27.4	24.5 ± 0.15,[a] 29.3 ± 0.15,[b] 29.6[c]	pC/N
d_{32}	−24.3	-19.5 ± 0.20,[a] −22.3[c]	pC/N
d_{31}	3.4	9.8 ± 0.07,[a] 18.5[c]	pC/N

[a]Reference 46.
[b]Reference 38.
[c]Reference 24.

cale domain structure and microstructure evolution. In the application of the ferroelectric materials, for instance, it can be used to investigate the ferroelectric properties especially the domain structures and their temporal evolutions, as well as the effects of substrate constraint on the phase transition temperatures and domains in ferroelectric materials such as $PbTiO_3$, $BaTiO_3$, PZT, etc. In order to model the real processes in the materials, the accurate thermodynamic and dynamic data should be determined as input parameters in the phase-field model. The stable microstructure is a direct consequence of minimizing the total energy of the system. The fitted thermodynamic free energy function as an intrinsic thermodynamic energy term in the total energy in the phase field model quantitatively determines the total energy of the system. The ferroelectric properties of $KNbO_3$ can thus be determined. It will have many straightforward, immediate, and important applications. For instance, one can study domain structures and wall motion in $KNbO_3$ single crystals, the domain structures and their evolution under applied fields such as pressure and electric field. Further, the substrate constraints effect on domain structures, phase transition temperatures as well as other ferroelectric properties for $KNbO_3$ thin film can also be investigated.

VI. SUMMARY

In summary, an eight-order polynomial of free energy function has been constructed in the framework of LGD phase transition theory for describing the ferroelectric properties of the potassium niobate ($KNbO_3$) single crystal. All of the free energy expansion coefficients are determined based on the related properties of $KNbO_3$. The fitted free energy function is used to model and predict the structural and ferroelectric properties of $KNbO_3$. These properties include the phase transition temperatures, spontaneous polarizations, entropy and latent heat changes, dielectric constants, spontaneous strains, and lattice constants. We also predicted the piezoelectric coefficients and phase transition temperature changes and dielectric constants under a hydrostatic pressure. The calculation results suggest that the free energy function describe well the properties of a $KNbO_3$ single crystal. The fitted free energy function can lead to many applications. For instance, it can be employed in the phase field model to simulate the domain evolution and ferroelectric properties for both $KNbO_3$ bulk and thin film.

[1]I. Biaggio, P. Kerkoc, L.-S. Wu, P. Gunter, and B. Zysset, J. Opt. Soc. Am. B **9**, 507 (1992).
[2]B. Zysset, I. Biaggio, and P. Günter, J. Opt. Soc. Am. B **9**, 380 (1992).
[3]K. Nakamura, T. Tokiwa, and Y. Kawamura, J. Appl. Phys. **91**, 9272 (2002).
[4]K. Yamanouchi, H. Odagawa, T. Kojima, and T. Matsumura, Electron. Lett. **33**, 193 (1997).
[5]H. Nagata and T. Takenaka, Jpn. J. Appl. Phys., Part 1 **36**, 6055 (1997).
[6]H. Nagata and T. Takenaka, Jpn. J. Appl. Phys., Part 1 **37**, 5311 (1998).
[7]A. F. Devonshire, Philos. Mag. **40**, 1040 (1949).
[8]Y. L. Li, L. E. Cross, and L. Q. Chen, J. Appl. Phys. **98**, 064101 (2005).
[9]A. J. Bell and L. E. Cross, Ferroelectrics **59**, 197 (1984).
[10]L. E. Cross, J. George, and A. Rossetti, J. Appl. Phys. **69**, 896 (1991).
[11]S. Triebwasser, Phys. Rev. **101**, 993 (1956).
[12]O. E. Kvyatkovski ĭ and G. A. Zakharov, Phys. Solid State **48**, 1034 (2006).
[13]W. Kleemann and F. J. Schäfer, Phys. Rev. B **30**, 1148 (1984).
[14]S. Dorfman, D. Fuks, A. Gordon, A. V. Postnikov, and G. Borstel, Phys. Rev. B **52**, 7135 (1995).
[15]Z. X. Shen, Z. P. Hu, T. C. Chong, C. Y. Beh, S. H. Tang, and M. H. Kuok, Phys. Rev. B **52**, 3976 (1995).
[16]D. Gourdain, P. Pruzan, J. M. Besson, S. Klotz, J. C. Chervin, and B. Canny, Phys. Rev. B **65**, 054104 (2002).
[17]M. M. Shamim and T. Ishidate, Solid State Commun. **113**, 713 (2000).
[18]P. Pruzan, D. Gourdain, J. C. Chervin, B. Canny, B. Couzinet, and M. Hanfland, Solid State Commun. **123**, 21 (2002).
[19]Y. Kobayashi, S. Endo, K. Deguchi, L. C. Ming, and G. Zou, Solid State Commun. **120**, 515 (2001).
[20]G. A. Samara and P. S. Peercy, Solid State Phys. **36**, 1 (1981).
[21]G. A. Samara, Ferroelectrics **73**, 145 (1987).
[22]D. Gourdain, E. Moya, J. C. Chervin, B. Canny, and P. Pruzan, Phys. Rev. B **52**, 3108 (1995).
[23]J. Hirohashi, K. Yamada, H. Kamio, M. Uchida, and S. Shichijyo, J. Appl. Phys. **98**, 034107 (2005).
[24]S. Wada, K. Muraoka, H. Kakemoto, T. Tsurumi, and H. Kumagai, Jpn. J. Appl. Phys., Part 1 **43**, 6692 (2004).
[25]L. Liang, Y. L. Li, L.-Q. Chen, S. Y. Hu, and G.-H. Lu, Appl. Phys. Lett. **94**, 072904 (2009).
[26]M. J. Haun, E. Furman, S. J. Jang, and L. E. Cross, Ferroelectrics **99**, 13 (1989).
[27]L. Lian, T. C. Chong, H. Kumagai, M. Hirano, L. Taijing, and S. C. Ng, J. Appl. Phys. **80**, 376 (1996).
[28]R. M. Cotts and W. D. Knight, Phys. Rev. **96**, 1285 (1954).
[29]H. Chaib, D. Khatib, A. Toumanari, and W. Kinase, J. Phys.: Condens. Matter **12**, 2317 (2000).
[30]E. Wiesendanger, Ferroelectrics **6**, 263 (1974).
[31]G. Shirane, H. Danner, A. Pavlovic, and R.Pepinsey, Phys. Rev. **93**, 672 (1954).
[32]Y. Watanabe, J. Appl. Phys. **83**, 2179 (1998).
[33]M. D. Fontana, G. Metrat, J. L. Servoin, and F. Fercais, J. Phys. C **17**, 483 (1984).
[34]K. S. Kam and J. H. Henkel, Ferroelectrics **34**, 143 (1981).
[35]R. Resta, M. Posternak, and A. Baldereschi, Phys. Rev. Lett. **70**, 1010 (1993).
[36]Y. Uematsu and T. Fukuda, Jpn. J. Appl. Phys. **10**, 507 (1971).
[37]A. E. Clement and G. C. Gilbreath, Appl. Opt. **30**, 2458 (1991).
[38]M. Zgonik, R. Schlesser, I. Biaggio, E. Voit, J. Tscheny, and P. Günter, J. Appl. Phys. **74**, 1287 (1993).
[39]J. H. Kim and C. S. Yoon, Appl. Phys. Lett. **81**, 3332 (2002).
[40]G. Shirane, R. Newnham, and R. Pepinsky, Phys. Rev. **96**, 581 (1954).
[41]S. Triebwasser and J. Halpern, Phys. Rev. **98**, 1562 (1955).
[42]M. Sepliarsky, S. R. Phillpot, D. Wolf, M. G. Stachiotti, and R. L. Migoni, Appl. Phys. Lett. **76**, 3986 (2000).
[43]Y. Kobayashi, S. Endo, T. Ashida, L. C. Ming, and T. Kikegawa, Phys. Rev. B **61**, 5819 (2000).
[44]N. A. Pertsev, A. G. Zembilgotov, and A. K. Tabantev, Phys. Rev. Lett. **80**, 1988 (1998).
[45]Y. L. Li, S. Y. Hu, Z. K. Liu, and L. Q. Chen, Acta Mater. **50**, 395 (2002).
[46]P. Günter, Jpn. J. Appl. Phys. **16**, 1727 (1977).
[47]I. Masuda, K.-I. Kakimoto, and H. Ohsato, J. Electroceram. **13**, 555 (2004).